

# Quantum Simulation of Bound-State-Enhanced Quantum Metrology

Cheng-Ge Liu,<sup>1,\*</sup> Cong-Wei Lu,<sup>1,\*</sup> Na-Na Zhang,<sup>2</sup> and Qing Ai<sup>1,†</sup>

<sup>1</sup>*Department of Physics, Applied Optics Beijing Area Major Laboratory,  
Beijing Normal University, Beijing 100875, China*

<sup>2</sup>*School of Optoelectronics Engineering, Chongqing University of Posts and Telecommunications, Chongqing 400065, China*  
(Dated: November 27, 2023)

Quantum metrology explores quantum effects to improve the measurement accuracy of some physical quantities beyond the classical limit. However, due to the interaction between the system and the environment, the decoherence can significantly reduce the accuracy of the measurement. Many methods have been proposed to restore the accuracy of the measurement in the long-time limit. Recently, it has been found that the bound state can assist the error-free measurement and recover the  $t^{-1}$  scaling [K. Bai, Z. Peng, H. G. Luo, and J. H. An, Phys. Rev. Lett. 123, 040402 (2019)]. Here, by using  $N$ -qubits, we propose a method to simulate the open quantum dynamics of the hybrid system including one atom and coupled resonators. We find that the error of the measurement can vanish as the time increases due to the existence of the bound state. By both analytical and numerical simulations, we prove the  $t^{-1}$  scaling of the measurement error can be recovered when there is a bound state in the hybrid system. Interestingly, we observe that there are perfect oscillations which can be used for the evaluation of the atomic transition frequency. For a finite- $N$ , the duration of the perfect oscillations doubles as one more qubit is involved.

## I. INTRODUCTION

Compared with classical metrology, quantum metrology can greatly improve the measurement accuracy and play a significant role in gravitational-wave detection [1–3] and quantum radar [4–6], atomic clocks [7–10], magnetometers [11–13], gravimeters [14, 15], navigation and biological monitoring [16–21], quantum biology [17–19] and so on.

According to the central-limit theorem [22, 23], by performing a large number of measurements, the error of the measurements will be reduced by a factor  $\sqrt{N}$  with  $N$  being the number of measurements, i.e., the shot-noise limit (SNL) or the standard quantum limit [23]. The quantum metrology explores quantum entanglement [24–26], coherence [27–29] and squeezing [30–32] to improve the accuracy of the measurement in order to reach the Heisenberg limit (HL) which scales as  $N^{-1}$ . As long as the system-bath interaction is present, the measurement of a specific physical quantity is inevitably affected by the error. The precision of the quantum metrology in a Markovian bath is reduced the SNL [33]. The SNL can also be defeated in non-Markovian noise and thus achieve the Zeno limit (ZL), i.e.,  $N^{-3/4}$  [34–36].

Ramsay spectrum is widely used in practical quantum metrology, which approaches the HL when the noise is absent [37]. However, in practice, since the system is open to the environment, the measurement accuracy of physical quantities will be affected by environmental noise. In the presence of Markovian pure-dephasing noise, the accuracy is reduced from the HL back to the SNL [33]. Although under non-Markovian noises the

accuracy can reach the Zeno limit, it is still lower than HL [35, 36, 38, 39]. In both cases, the measurement error will diverge over time. In order to improve the measurement accuracy, many methods have been proposed, such as purification [40], error correction [41–43], non-degenerate measurements [44], and bound states outside continuum [23, 45]. None of these proposals recover the HL and especially fail to resolve the issue of error diverging over time. It is natural to ask the question how to restore the measurement error without diverging over time?

Recent studies have shown that when there is a bound state in the open quantum system, it allows the measurement precision to beat the SNL and recover the ZL over long encoding times [45]. On the other hand, we notice that the hybrid system including few atoms and the coupled cavity array has been extensively studied in the past decade. It can be used for single-photon switch [46, 47], quantum transistors [48], routers [49], supercavity [50], non-reciprocal optics [51], and frequency converters [52]. Inspired by these discoveries, in this paper, we propose a scheme to simulate the open quantum dynamics of an atom in a coupled resonators. Here, the coupled resonators form a structured bath with the energy band centered at the cavity frequency and bandwidth 4 times the inter-cavity coupling. When the atomic transition frequency lies within the energy band of the bath, there emerges a bound state. In this case, if we measure the probability of the atom at the excited state, we can obtain an error-free measurement of the atomic transition frequency. In other words, the standard deviation of the measured atomic transition frequency scales  $t^{-1}$ . As the time approaches infinity, the error of the measurement vanishes. Our approach may pave the way for the quantum simulation of abundant physical phenomena in the hybrid system including few atoms and coupled resonators.

This paper is organized as follows. In the next

\* These authors contributed equally to this work.

† [aiqing@bnu.edu.cn](mailto:aiqing@bnu.edu.cn)

section, we will introduce our simulation scheme. By using  $N$ -qubits, we can effectively simulate the quantum dynamics of one atom and  $2^N - 1$  coupled cavities. We also provide the probability of the atomic excited state and the standard deviation of the measured atomic transition frequency, of which the detailed derivations are respectively shown in Appendixes A,B. Then, in Sec. III, we use the direct mapping method, which is given in Appendix C, to numerically simulate the dynamics of the atomic excited state. We explore the relation between the duration of the perfect oscillation and the number of cavities. We also use both analytical and numerical methods to verify that the error of the measurement decreases over time in the presence of a bound state. In Sec. IV, we summarize our main findings.

## II. SCHEME

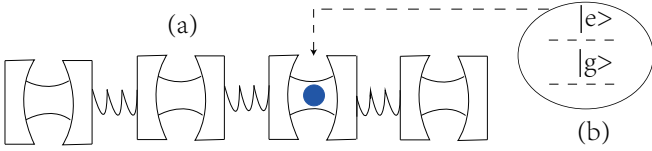


FIG. 1. Schematic illustration of a two-level atom and a coupled-cavity array. (a) Structure of coupled cavities, (b) a two-level atom.

We consider the interaction between a two-level atom and a coupled-cavity array [53]. As shown in Fig. 1, the Hamiltonian of the system reads

$$H = H_0 + H_c + H_I, \quad (1)$$

$$H_0 = \Omega|e\rangle\langle e|, \quad (2)$$

$$H_c = \omega_0 \sum_j a_j^\dagger a_j - \xi \sum_j (a_j^\dagger a_{j+1} + a_{j+1}^\dagger a_j), \quad (3)$$

$$H_I = J \sum_j (a_0^\dagger \sigma_+ + a_0 \sigma_-), \quad (4)$$

where  $\Omega$  is the transition frequency of the atom,  $a_j^\dagger$  ( $a_j$ ) represents create (annihilate) a photon with frequency  $\omega_0$  in the  $j$ th cavity,  $\xi$  is the coupling constant between two adjacent resonators,  $\sigma_+ = |e\rangle\langle g| = \sigma_-^\dagger$  is the raising operator of the atom with  $|e\rangle$  and  $|g\rangle$  being the excited and ground state of the atom respectively,  $J$  is the coupling constant between the atom and the 0th cavity. In this article, we have assumed  $\hbar = 1$  for simplicity.

Assuming the periodical boundary condition, by Fourier transformation, i.e.,  $a_j^\dagger = \sum_k a_k^\dagger e^{ikj}/\sqrt{N}$ , the total Hamiltonian (1) can be rewritten as

$$H = \sum_k \omega_k a_k^\dagger a_k + \Omega|e\rangle\langle e| + \sum_k J_k (a_k^\dagger \sigma_- + \text{H.c.}), \quad (5)$$

where  $\omega_k = \omega_0 - 2\xi \cos(k)$ ,  $J_k = J/\sqrt{N}$ . Since the total excitation  $N = \sum_k a_k^\dagger a_k + |e\rangle\langle e|$  is conserved, i.e.,

$[H, N] = 0$ , we assume that at time  $t$  the system is in the state  $|\psi(t)\rangle = \alpha(t)|v, e\rangle + \sum_k \beta_k(t) a_k^\dagger |v, g\rangle$  with  $|v\rangle$  being the vacuum state of all cavities. According to the Schrödinger equation, we have

$$i\dot{\alpha} = \Omega\alpha + \sum_k J_k \beta_k, \quad (6)$$

$$i\dot{\beta}_k = \omega_k \beta_k + J_k \alpha, \quad (7)$$

where the initial condition is given as  $\alpha(0) = 1$ ,  $\beta_k(0) = 0$ . As shown in Appendix A, we can obtain the analytic expression of the probability amplitude of the excited state of the atom as

$$\alpha(t) = A_1 e^{p_1 t} + A_2 e^{p_2 t} + \int_{-2\xi}^{2\xi} C(x) e^{i(x-\omega_0)t} dx, \quad (8)$$

where  $A_j$ 's ( $j = 1, 2$ ) are real,  $p_j$ 's ( $j = 1, 2$ ) are imaginary, The explicit expressions of all these parameters including  $C(x)$  can be referred to Appendix A. Since the last term of Eq. (8) decays exponentially in the long-time limit, the probability of the excited state of the atom reads

$$P_e = |\alpha(\infty)|^2 = A_1^2 + A_2^2 + 2A_1 A_2 \cos(\phi t), \quad (9)$$

where  $\phi = ip_2^* - ip_1$ . In order to measure the atomic transition frequency precisely, the variance is determined by the quantum Fisher information  $F(\Omega)$  as [28, 54, 55]

$$\delta\Omega^2 = \frac{1}{(T/t)F(\Omega)}, \quad (10)$$

$$F(\Omega) \equiv \frac{1}{P_e(1-P_e)} \left( \frac{\partial P_e}{\partial \Omega} \right)^2, \quad (11)$$

where  $T$  is the total duration of the experiment which is separated into repetition with each duration  $t$ . By the perturbation theory as shown in Appendix B, we have

$$\phi = 2\omega_0 - 2 \frac{\omega_0 - \Omega}{[(\omega_0 - \Omega)^2 - 4\xi^2]^2} J^4. \quad (12)$$

By substituting Eqs. (9), (11), (12) into Eq. (10), we can obtain the uncertainty of the atomic transition frequency as

$$\delta\Omega^2 = \frac{4t\xi^2 B_1 B_2}{J^{16} T B_3}, \quad (13)$$

where

$$B_1 = -\frac{J^8}{4\Omega_-^6 \xi^2} - \frac{J^8}{4\Omega_+^6 \xi^2} + \frac{J^8 \cos(\phi t)}{2\Omega_-^3 \Omega_+^3 \xi^2} + 1, \quad (14)$$

$$B_2 = \frac{J^8}{4\Omega_-^6} + \frac{J^8}{4(\Omega_+)^6} - \frac{J^8 \cos(\phi t)}{2\Omega_-^3 \Omega_+^3}, \quad (15)$$

$$B_3^{1/2} = \frac{2J^4 t [4\xi^2 + 3(\Omega - \omega_0)^2] \sin(\phi t)}{\Omega_-^6 \Omega_+^6} - \frac{3}{\Omega_-^7} - \frac{3}{\Omega_+^7} + \frac{3 \cos(\phi t)}{\Omega_-^4 \Omega_+^3} + \frac{3 \cos(\phi t)}{\Omega_-^3 \Omega_+^4}, \quad (16)$$

with  $\Omega_\pm = \pm 2\xi + \omega_0 - \Omega$ .

### III. NUMERICAL SIMULATION AND DISCUSSION

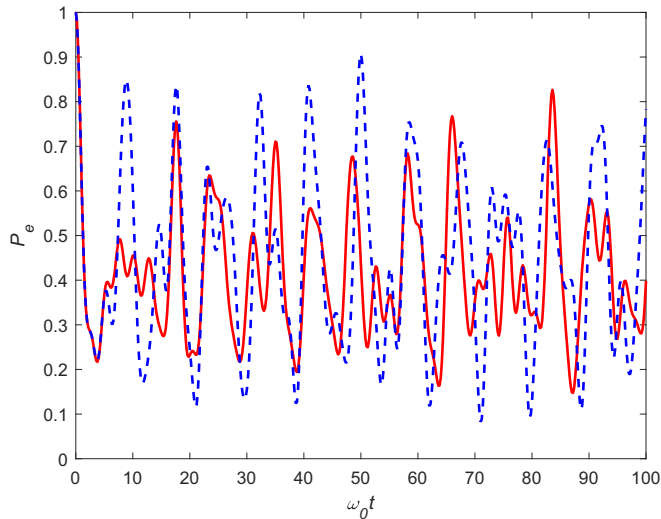


FIG. 2. The population dynamics  $P_e(t)$  of atomic excited state with small  $N$ 's, e.g. 3 qubits (blue dashed line) and 4 qubits (red solid line). Here, the parameters used in the calculation are  $\Omega = 2\omega_0$ ,  $J = 0.7\omega_0$  and  $\xi = 0.5\omega_0$ .

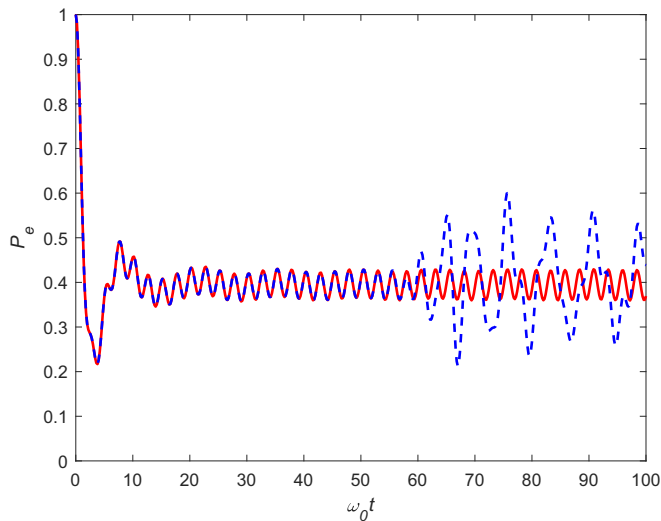


FIG. 3. The population dynamics  $P_e(t)$  of atomic excited state with larger  $N$ 's, e.g.  $N = 6$  (blue dashed line) and  $N = 7$  (red solid line). Here, the parameters are the same as Fig. 2.

As shown in Appendix C, we utilize  $N$  qubits to effectively simulate the quantum dynamics for one atom interacting with  $2^N - 1$  coupled resonators in the single-excitation subspace. In Fig. 2, it is shown that when the number of qubits  $N$  is relatively small, e.g.  $N = 3, 4$ , the population of the atom at the excited state  $P_e(t)$  does not oscillate with a specific frequency, and thus

does not provide any information for the frequency of the atom. However, if  $N$  is increased, e.g.  $N = 6, 7$  in Fig. 3, we find that there are persistent oscillations in  $P_e(t)$ , which indicates that there exists a bound state in the atom interacting with the cavity array. The underlying physical mechanism can be well explained by the analytical solution obtained in the previous section. At the beginning, due to the third term in Eq. (8),  $P_e(t)$  oscillates out of order. As the time passes by, since the contribution from the branch cut vanishes,  $P_e(t)$  oscillates with a specific frequency, as predicted by Eq. (9). By measuring this frequency, we effectively obtain the atomic transition frequency. Notice that this perfect oscillation does not last for ever. Interestingly, the duration of this perfect oscillation seems to get longer as  $N$  increases.

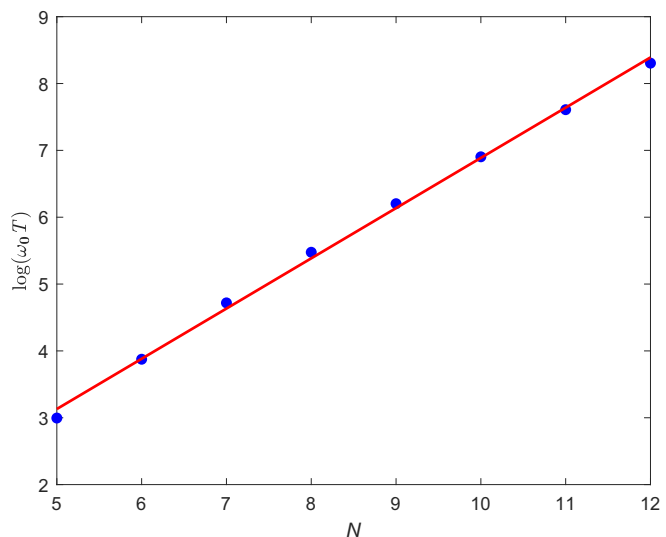


FIG. 4. The duration of the oscillation as a function of the number of qubits  $N$ . We use the function  $\log(\omega_0 T) = 0.75137 \times N - 0.62597$  (red solid line) to fit the data (blue dots) with the linear correlation coefficient  $r = 0.99$ . The other parameters are the same as Fig. 2.

In order to study the relation between the duration of perfect oscillation  $T$  and the number of qubits  $N$ , we plot  $\log(\omega_0 T)$  vs  $N$  in Fig. 4. By a linear fitting with the linear correlation coefficient  $r = 0.99$ , we show that  $\omega_0 T = \exp(0.75137 \times N - 0.62597)$ , which implies that the duration of the perfect oscillation doubles as we use one more qubit, i.e.,  $\exp(0.75137) \simeq 2.1199$ . Thus, when  $N$  approaches infinity, the coding time can be infinite, and we can obtain a perfect measurement of the atomic transition frequency, cf. Eq. (10). As shown in the figures below, we apply both the analytical and numerical methods to confirm our conjecture.

In Fig. 5, we show the uncertainty of atomic transition frequency  $\delta\Omega$  by Eq. (13) when the atomic transition frequency is within the band of the coupled resonators. At first,  $\delta\Omega$  experiences a rapid rise and followed a slow decay, guaranteeing the recovery of

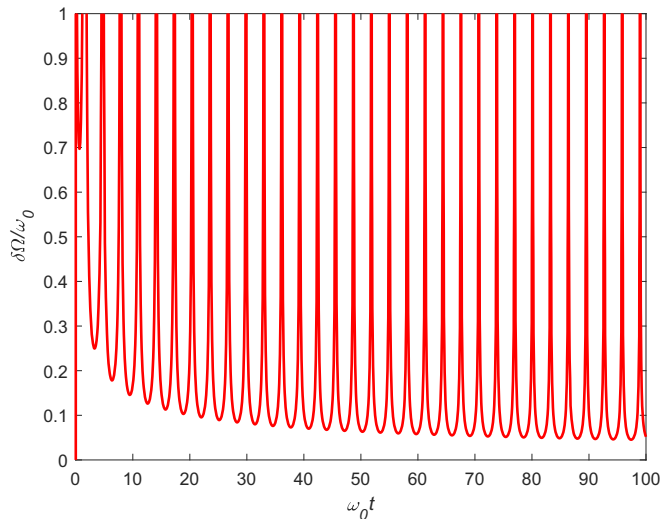


FIG. 5. The uncertainty  $\delta\Omega$  vs time with the atomic transition frequency within the band of the coupled resonators. The data is obtained by Eq. (13) with the following parameters, i.e.,  $\Omega = \omega_0$ ,  $g = 0.7\omega_0$ ,  $\xi = 0.7\omega_0$ , and  $\omega_0 T = 10^4$ .

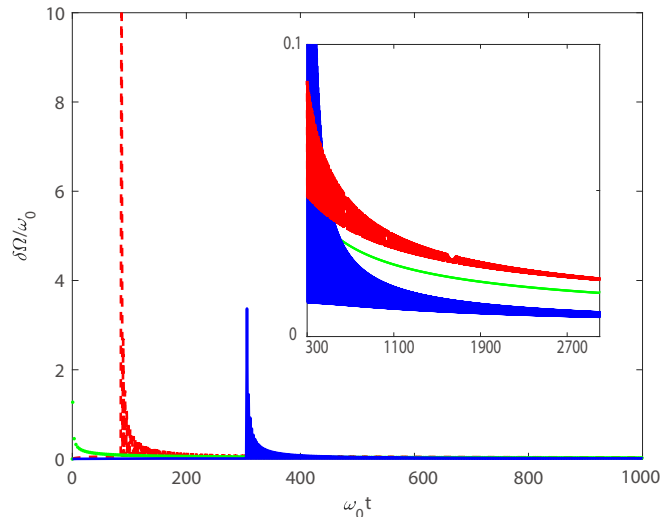


FIG. 6. The uncertainty  $\delta\Omega$  vs time for the different atomic transition frequencies, all within the band of the coupled resonators with dotted green line for  $\Omega = \omega_0$ , dashed red line for  $\Omega = 1.4\omega_0$ , solid blue line for  $\Omega = 1.8\omega_0$ . The data is obtained by Eq. (13) with the following parameters, i.e.,  $J = 0.7\omega_0$ ,  $\xi = 0.7\omega_0$ , and  $\omega_0 T = 10^3$ .

vanishing measurement error. In order to investigate the dependence of  $\delta\Omega$  on  $\Omega$ , we plot the dynamics of  $\delta\Omega$  for different  $\Omega$ 's in Fig. 6. If we tune the atomic transition frequency to depart from the center of the band, the sharp rise will be delayed. In addition, it will take longer to recover the error-free measurement. Especially when  $\Omega = \omega_0$ , i.e., at the center of the band, it is found that the uncertainty approaches to the noiseless case with the fastest rate. Notice that in obtaining Eq. (13) we

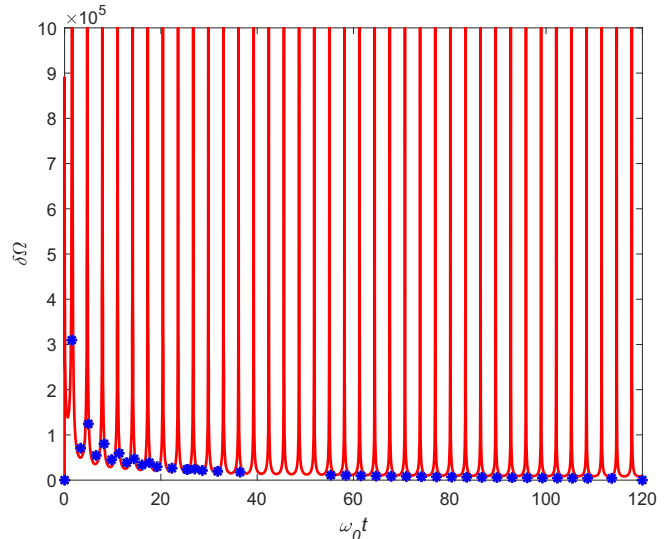


FIG. 7. Comparison of analytical and numerical results for the uncertainty  $\delta\Omega$  vs time. The data is obtained by analytical Eq. (13) (solid red line) and numerical solution (blue stars) with the following parameters, i.e.,  $N = 8$ ,  $\Omega = \omega_0$ ,  $J = 0.3\omega_0$ ,  $\xi = \omega_0$ , and  $\omega_0 T = 120$ .

assume that the atom-resonator coupling  $J$  is weak, i.e.,  $|\omega_0 \pm 2\xi|, \Omega \gg J$ , and the atomic transition frequency is within the band of the coupled resonators, i.e.,  $\Omega \in [\omega_0 - 2\xi, \omega_0 + 2\xi]$ . In order to verify the above assumption is valid, we compare the approximated Eq. (13) with numerically-exact Eq. (10) in Fig. 7. Obviously, both two solutions agree very well with each other and thus suggests reliable approximations by Eq. (13). However, due to the limitation of the approximations of the analytical method, we can not effectively simulate the situation with the atomic transition frequency beyond the band by Eq. (13). Here, in Fig. 8, we plot the dynamics of the measured atomic transition frequency by Eq. (10) with the parameters being  $N = 8$ ,  $\Omega = \omega_0$ ,  $J = 0.3\omega_0$ ,  $\xi = \omega_0$ , and  $\omega_0 T = 120$ . As shown, after an increase about  $\omega_0 t = 5$ ,  $\delta\Omega$  achieves a steady state although there still exist oscillations with small amplitude. It does not recover the  $1/t$  measurement because there does not exist the bound state.

#### IV. CONCLUSION

To conclude, we study the effects of the bound state on the quantum metrology in an atom interacting with coupled resonators. In the hybrid system with finite number  $n$  of cavities, we find that when the number of qubits is large enough, e.g.  $n \geq 2^5 - 1 = 31$ , there exist perfect oscillations in the population dynamics of the atomic excited state, which may be used for the evaluation of the atomic transition frequency. The duration of these perfect oscillations is linear with respect to  $n$ . As  $n$  approaches infinity, we can recover the

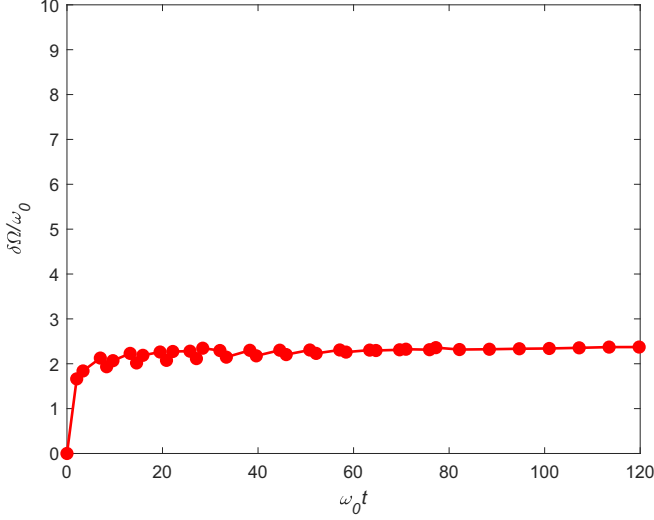


FIG. 8. Numerical simulation of the uncertainty  $\delta\Omega$  vs time with the measured atom transition frequency beyond the band of the coupled resonators. The data is obtained by Eq. (10) with the following parameters, i.e.,  $N = 8$ ,  $\Omega = 8\omega_0$ ,  $J = 0.3\omega_0$ ,  $\xi = \omega_0$ , and  $\omega_0 T = 120$ .

noiseless metrology. These perfect oscillations indicate that there exists a bound state in the hybrid system. Their duration lasts for a finite time because there are finite cavities, i.e., finite bath modes. By numerical simulations, we can prove that the bound state exists when the atomic transition frequency is within the energy band of the coupled resonators. In addition to the numerical simulations, we obtain an analytical result of the uncertainty of the atomic transition frequency for small atom-cavity interaction strength when the bound state is present. It indicates that the error-free measurement is recovered with infinite cavities in the long-time limit due to the existence of the bound state. The results suggest that the non-Markovian effects and the bound state account for the high accuracy of the quantum metrology. Our research may shed light on the design of the hybrid system exploring the bound state for quantum metrology.

#### ACKNOWLEDGMENTS

This work is supported by Beijing Natural Science Foundation under Grant No. 1202017 and the National Natural Science Foundation of China under Grant Nos. 11674033, 11505007, and Beijing Normal University under Grant No. 2022129, Scientific and Technological Research Program of Chongqing Municipal Education Commission under Grant No. KJQN202200603, and Chongqing University of Posts and Telecommunications under Grant No. A2022-304.

#### Appendix A: Population of Atomic Excited State

After the Fourier transformation, the total Hamiltonian reads [56]

$$H = \sum_k \omega_k a_k^\dagger a_k + \Omega |e\rangle \langle e| + \sum_k J_k (a_k^\dagger \sigma_- + \text{h.c.}) \quad (\text{A1})$$

In the subspace of single excitation, we assume the wavefunction as

$$|\psi\rangle = \alpha(t) |0, e\rangle + \sum_k \beta_k(t) |k, g\rangle. \quad (\text{A2})$$

By substituting Eqs. (A2) and (A1) into the Schrödinger equation, we can obtain

$$i\dot{\alpha}(t) = \Omega\alpha(t) + \sum_k J_k \beta_k(t), \quad (\text{A3})$$

$$i\dot{\beta}_k(t) = \omega_k \beta_k(t) + J_k \alpha(t), \quad (\text{A4})$$

where  $\alpha(0) = 1$ ,  $\beta_k(0) = 0$  are the initial condition of the system. Then, we perform the Laplace transform on Eqs. (A3) and (A4) to have

$$i(p\tilde{\alpha}(p) - 1) = \Omega\tilde{\alpha}(p) + \sum_k J_k \tilde{\beta}_k(p), \quad (\text{A5})$$

$$ip\tilde{\beta}_k(p) = \omega_k \tilde{\beta}_k(p) + J_k \tilde{\alpha}(p). \quad (\text{A6})$$

After some algebra, we can calculate the probability amplitude of the excited state in  $p$ -space as

$$\tilde{\alpha}(p) = \frac{1}{p + i\Omega + \sum_k \frac{J_k^2}{p + i\omega_k}}. \quad (\text{A7})$$

After the inverse Laplace transformation, we can obtain the probability amplitude of the excited state in the time domain as

$$\alpha(t) = \frac{1}{2\pi i} \int_{\sigma - i\infty}^{\sigma + i\infty} dp \tilde{\alpha}(p) e^{pt}. \quad (\text{A8})$$

Using the residual theorem, we have

$$\begin{aligned} \alpha(t) = & -\frac{1}{2\pi i} \left( \int_{C_R} \tilde{\alpha}(p) e^{pt} + \int_{l_1} \tilde{\alpha}(p) e^{pt} + \int_{l_2} \tilde{\alpha}(p) e^{pt} \right) \\ & + \sum_{j=1}^2 \text{res}(\tilde{\alpha}(p_j) e^{p_j t}), \end{aligned} \quad (\text{A9})$$

where  $C_R$  is the large semicircle at the infinite,  $p_j$ 's and  $l_j$ 's ( $j = 1, 2$ ) are respectively the two singularities and two branch lines which are given by

$$p + i\Omega + \sum_k \frac{J_k^2}{p + i\omega_k} = 0. \quad (\text{A10})$$

According to Eq. (A10), the branch lines are defined by  $p + i\omega_k = 0$ , i.e.,  $p \in [ip_m, ip_M]$ , where  $p_m = -\omega_0 - 2\xi$ ,  $p_M = -\omega_0 + 2\xi$ . Notice that

$$\sum_k \frac{J_k^2}{p + i\omega_k} = \frac{J^2}{2\pi\xi} \oint_{|z|=1} dz \frac{1}{z^2 + Mz + 1}, \quad (\text{A11})$$

where  $M = (ip - \omega_0)/\xi$ ,  $z_{\pm} = (-M \pm \sqrt{M^2 - 4})/2$  are the two singularities. In other words,  $p \notin [-i(\omega_0 + 2\xi), -i(\omega_0 - 2\xi)]$ , i.e.,  $M > 2$  or  $M < -2$ . In the former case, since  $ip > \omega_0 + 2\xi$ ,  $-1 < z_+ < 0$ ,  $z_- < -1$ , we have

$$\frac{J^2}{2\pi\xi} \oint_{|z|=1} dz \frac{1}{z^2 + Mz + 1} = \frac{iJ^2}{\xi\sqrt{M^2 - 4}}. \quad (\text{A12})$$

By substituting Eq. (A12) into Eq. (A10), we can obtain

$$p + i\Omega + i \frac{J^2}{\xi\sqrt{M^2 - 4}} = f_1(p). \quad (\text{A13})$$

Through  $f_1(p_1) = 0$  and  $ip_1 > \omega_0 + 2\xi$ , we attain the first singularity. In the same way, for the case of  $M < -2$ , since

$$\frac{J^2}{2\pi\xi} \oint_{|z|=1} \frac{dz}{z^2 + Mz + 1} = -\frac{iJ^2}{\xi\sqrt{M^2 - 4}}, \quad (\text{A14})$$

we have

$$p + i\Omega - i \frac{J^2}{\xi\sqrt{M^2 - 4}} = f_2(p). \quad (\text{A15})$$

By  $f_2(p_2) = 0$  and  $ip_2 < \omega_0 - 2\xi$ , we can obtain the second singularity. As a result, the contribution from the singularities in Eq. (A9) reads

$$\text{res}(\tilde{\alpha}(p_j)e^{p_j t}) = A_j e^{p_j t}, \quad (\text{A16})$$

where  $A_j = \left(\frac{df_j}{dp}\bigg|_{p_j}\right)^{-1}$ .

Thanks to Jordan Lemma, we know  $\int_{C_R} \tilde{\alpha}(p)e^{pt} = 0$ . Thus, we have

$$\begin{aligned} & -\frac{1}{2\pi i} \left( \int_{l_1} \tilde{\alpha}(p)e^{pt} + \int_{l_2} \tilde{\alpha}(p)e^{pt} dp \right) \\ &= -\frac{1}{2\pi i} \left( \int_{p_m}^{p_M} \frac{e^{ipt}}{p + \Omega - \sum_k \frac{g_k^2}{p + \omega_k + i0^+}} dp \right. \\ & \quad \left. + \int_{p_M}^{p_m} \frac{e^{ipt}}{p + \Omega - \sum_k \frac{J_k^2}{p + \omega_k - i0^+}} dp \right). \quad (\text{A17}) \end{aligned}$$

Here,

$$\begin{aligned} & \sum_k \frac{J_k^2}{p + i\omega_k \pm i0^+} \\ &= \frac{J^2}{2\pi} \left[ \mp \frac{i2\pi}{\sqrt{4\xi^2 - (\omega_0 + p)^2}} + \int_{-\pi}^{\pi} dk P\left(\frac{1}{p + \omega_k}\right) \right], \quad (\text{A18}) \end{aligned}$$

where  $P(x)$  is the principal value function. Since

$$\int_{-\pi}^{\pi} dk P\left(\frac{1}{p + \omega_k}\right) = 0, \quad (\text{A19})$$

by substituting Eq. (A18) into Eq. (A17), we have

$$-\frac{1}{2\pi i} \left( \int_{l_1} \tilde{\alpha}(p)e^{pt} + \int_{l_2} \tilde{\alpha}(p)e^{pt} dp \right) = \int_{-2\xi}^{2\xi} C(x)e^{i(x-\omega_0)t} dx, \quad (\text{A20})$$

where  $C(x) = (g^2 \sqrt{4\xi^2 - x^2})/[(\Omega - \omega_0 + x)^2(4\xi^2 - (x)^2) + g^4]$ . Finally, we obtain the probability amplitude of the atomic excited state as

$$\alpha(t) = A_1 e^{p_1 t} + A_2 e^{p_2 t} + \int_{-2\xi}^{2\xi} C(x)e^{i(x-\omega_0)t} dx \quad (\text{A21})$$

where

$$A_1 = \frac{-4\xi^2 + (ip_1 - \omega_0)^2}{-4\xi^2 + (ip_1 - \omega_0)^2 + (ip_1 - \Omega)(ip_1 - \omega_0)} \quad (\text{A22})$$

$$A_2 = \frac{(ip_2 - \omega_0)^2 - 4\xi^2}{(ip_2 - \omega_0)^2 - 4\xi^2 + (ip_2 - \Omega)(ip_2 - \omega_0)}. \quad (\text{A23})$$

After some algebra, we find that  $p_j$ 's ( $j = 1, 2$ ) are pure imaginary numbers.

## Appendix B: Uncertainty by perturbation

In order to obtain the uncertainty of  $\Omega$ , we shall first of all determine  $p_1$  and  $p_2$  in Eq. (A21) by perturbation theory. Take advantage of Eqs. (A13) and (A15), we have

$$(ip - \Omega)^2 [(ip - \omega_0)^2 - 4\xi^2] = J^4, \quad (\text{B1})$$

By the perturbation theory, to the zeroth order of  $J^4$ , we can obtain

$$(x - \Omega)^2 [(x - \omega_0)^2 - 4\xi^2] = 0, \quad (\text{B2})$$

where  $x = ip$ . There are four solutions to the above equation, i.e.,

$$x_{01} = \omega_0 + 2\xi, \quad (\text{B3})$$

$$x_{02} = \omega_0 - 2\xi, \quad (\text{B4})$$

$$x_{03} = x_{04} = \Omega. \quad (\text{B5})$$

In the following, we will obtain the solutions to Eq. (B1) to the first order of  $J^4$ .

As shown in Appendix A, i.e.,  $ip_1 > 2\xi + \omega_0$  and  $ip_2 < -2\xi + \omega_0$ , only  $x_1$  and  $x_2$  are kept for the following discussions. To the first order of  $g^4$ , we assume  $x_j = x_{0j} + C_j g^4$  ( $j = 1, 2, 3, 4$ ). Substitute them back into Eq. (B1), we can obtain

$$(x - \Omega)^2 (x - x_{01})(x - x_{02}) = J^4. \quad (\text{B6})$$

Thus, we have

$$C_1 = \frac{1}{4\xi\Omega_+^2}, \quad (\text{B7})$$

$$C_2 = \frac{-1}{4\xi\Omega_-^2}. \quad (\text{B8})$$

where  $\Omega_{\pm} = \pm 2\xi + \omega_0 - \Omega$ . In all,  $p_1 = -ix_1$  and  $p_2 = -ix_2$ .

Having known the analytical expressions of  $p_j$ 's, in the long-time limit, the population of the atom in the excited state reads

$$P_e = |\alpha(\infty)|^2 = A_1^2 + A_2^2 + 2A_1 A_2 \cos(\phi t), \quad (\text{B9})$$

where  $\phi = x_2 + x_1$ , the contribution from the integral term in Eq. (A21) vanishes when the time is large enough. By substituting  $p_1$  and  $p_2$  into Eqs. (A22) and (A23), we have

$$A_1 = \frac{J^4}{2\Omega_+^3 \xi}, \quad (\text{B10})$$

$$A_2 = -\frac{J^4}{2\Omega_-^3 \xi}, \quad (\text{B11})$$

$$\phi = 2\omega_0 + (C_3 + C_4)J^4. \quad (\text{B12})$$

The uncertainty of the atomic transition frequency is written as

$$\delta\Omega^2 = \frac{1}{(T/t)F(\Omega)}, \quad (\text{B13})$$

where the Fisher information  $F(\Omega)$  is

$$F(\Omega) \equiv \frac{1}{P_e(1-P_e)} \left( \frac{\partial P_e}{\partial \Omega} \right)^2. \quad (\text{B14})$$

According to Eqs. (B13), (B14), (B9), the uncertainty is explicitly given as

$$\delta\Omega^2 = \frac{4t\xi^2 B_1 B_2}{J^{16} T B_3}, \quad (\text{B15})$$

where

$$B_1 = -\frac{J^8}{4\Omega_-^6 \xi^2} - \frac{J^8}{4\Omega_+^6 \xi^2} + \frac{J^8 \cos(\phi t)}{2\Omega_-^3 \Omega_+^3 \xi^2} + 1, \quad (\text{B16})$$

$$B_2 = \frac{J^8}{4\Omega_-^6} + \frac{J^8}{4(\Omega_+)^6} - \frac{J^8 \cos(\phi t)}{2\Omega_-^3 \Omega_+^3}, \quad (\text{B17})$$

$$B_3^{1/2} = \frac{2J^4 t [4\xi^2 + 3(\Omega - \omega_0)^2] \sin(\phi t)}{\Omega_-^6 \Omega_+^6} - \frac{3}{\Omega_-^7} - \frac{3}{\Omega_+^7} + \frac{3 \cos(\phi t)}{\Omega_-^4 \Omega_+^3} + \frac{3 \cos(\phi t)}{\Omega_-^3 \Omega_+^4}. \quad (\text{B18})$$

## Appendix C: Direct Mapping

In this section, we discuss how to demonstrate the bound-state enhanced metrology by the quantum simulation approach with finite number of qubits. We focus our investigation in the single-excitation subspace. If we use  $N$  qubits for quantum simulation, the dimension of the Hilbert space is  $2^N$ . For example, when  $N = 2$ , we perform the following mapping before quantum simulation, i.e.,

$$|00\rangle = |0\rangle|e\rangle, \quad (\text{C1})$$

$$|01\rangle = a_1^\dagger |0\rangle|g\rangle, \quad (\text{C2})$$

$$|10\rangle = a_2^\dagger |0\rangle|g\rangle, \quad (\text{C3})$$

$$|11\rangle = a_3^\dagger |0\rangle|g\rangle, \quad (\text{C4})$$

where  $|g\rangle$  ( $|e\rangle$ ) the atomic ground (excited) state,  $|0\rangle$  is the vacuum state of all cavities,  $a_j^\dagger |0\rangle$  indicates that there is one photon in the  $j$ th cavity while all other cavities are in the vacuum state. Therefore, by using  $N$  qubits, we can effectively simulation the quantum dynamics of one atom plus number  $2^N - 1$  coupled cavities.

- 
- [1] H. Grote, K. Danzmann, K. L. Dooley, R. Schnabel, J. Slutsky, and H. Vahlbruch, "First long-term application of squeezed states of light in a gravitational-wave observatory," *Phys. Rev. Lett.* **110**, 181101 (2013).
- [2] R. Schnabel, N. Mavalvala, D. E. McClelland, and P. K. Lam, "Quantum metrology for gravitational wave astronomy," *Nat. Commun.* **1**, 121 (2010).
- [3] The LIGO Scientific Collaboration, "A gravitational wave observatory operating beyond the quantum shot-noise limit," *Nat. Phys.* **7**, 962 (2011).
- [4] S. Barzanjeh, S. Guha, C. Weedbrook, D. Vitali, J. H. Shapiro, and S. Pirandola, "Microwave quantum illumination," *Phys. Rev. Lett.* **114**, 080503 (2015).
- [5] L. Maccone and C. L. Ren, "Quantum radar," *Phys. Rev. Lett.* **124**, 200503 (2020).
- [6] G. Arrad, Y. Vinkler, D. Aharonov, and A. Retzker, "Increasing sensing resolution with error correction," *Phys. Rev. Lett.* **112**, 150801 (2014).
- [7] I. Kruse, K. Lange, J. Peise, B. Lücke, L. Pezzè, J. Arlt, W. Ertmer, C. Lisdat, L. Santos, A. Smerzi, and C. Klempt, "Improvement of an atomic clock using squeezed vacuum," *Phys. Rev. Lett.* **117**, 143004 (2016).
- [8] O. Hosten, N. J. Engelsen, R. Krishnakumar, and M. A. Kasevich, "Measurement noise 100 times lower than the quantum-projection limit using entangled atoms," *Nature* **529**, 505 (2016).
- [9] L. Pezzè and A. Smerzi, "Heisenberg-limited noisy atomic clock using a hybrid coherent and squeezed state protocol," *Phys. Rev. Lett.* **125**, 210503 (2020).
- [10] R. Kaubruegger, D. V. Vasilyev, M. Schulte, K. Hammerer, and P. Zoller, "Quantum variational optimization of Ramsey interferometry and atomic clocks," *Phys. Rev. X* **11**, 041045 (2021).
- [11] L. Thiel, D. Rohner, M. Ganzhorn, P. Appel, E. Neu, B. Müller, R. Kleiner, D. Koelle, and P. Maletinsky, "Quantitative nanoscale vortex imaging using a cryogenic

- quantum magnetometer,” *Nat. Nanotechnol.* **11**, 677 (2016).
- [12] J. M. Taylor, P. Cappellaro, L. Childress, L. Jiang, D. Budker, P. R. Hemmer, A. Yacoby, R. Walsworth, and M. D. Lukin, “High-sensitivity diamond magnetometer with nanoscale resolution,” *Nat. Phys.* **4**, 810 (2008).
- [13] H. Bao, J. L. Duan, S. C. Jin, X. D. Lu, P. X. Li, W. Z. Qu, M. F. Wang, I. Novikova, E. E. Mikhailov, K. F. Zhao, K. Mølmer, H. Shen, and Y. H. Xiao, “Spin squeezing of  $10^{11}$  atoms by prediction and retrodiction measurements,” *Nature* **581**, 159 (2020).
- [14] K. S. Hardman, P. J. Everitt, G. D. McDonald, P. Manju, P. B. Wigley, M. A. Sooriyabandara, C. C. N. Kuhn, J. E. Debs, J. D. Close, and N. P. Robins, “Simultaneous precision gravimetry and magnetic gradiometry with a Bose-Einstein condensate: A high precision, quantum sensor,” *Phys. Rev. Lett.* **117**, 138501 (2016).
- [15] P. Asenbaum, C. Overstreet, T. Kovachy, D. D. Brown, J. M. Hogan, and M. A. Kasevich, “Phase shift in an atom interferometer due to spacetime curvature across its wave function,” *Phys. Rev. Lett.* **118**, 183602 (2017).
- [16] J. M. Cai and M. B. Plenio, “Chemical compass model for avian magnetoreception as a quantum coherent device,” *Phys. Rev. Lett.* **111**, 230503 (2013).
- [17] M. A. Taylor and W. P. Bowen, “Quantum metrology and its application in biology,” *Phys. Rep.* **615**, 1 (2016).
- [18] A. Crespi, M. Lobino, J. C. F. Matthews, A. Politi, C. R. Neal, R. Ramponi, R. Osellame, and J. L. O’Brien, “Measuring protein concentration with entangled photons,” *Appl. Phys. Lett.* **100**, 233704 (2012).
- [19] M. A. Taylor, J. Janousek, V. Daria, J. Knittel, B. Hage, H.-A. Bachor, and W. P. Bowen, “Subdiffraction-limited quantum imaging within a living cell,” *Phys. Rev. X* **4**, 011017 (2014).
- [20] C. Y. Cai, Q. Ai, H. T. Quan, and C. P. Sun, “Sensitive chemical compass assisted by quantum criticality,” *Phys. Rev. A* **85**, 022315 (2012).
- [21] L. P. Yang, Q. Ai, and C. P. Sun, “Generalized Holstein model for spin-dependent electron-transfer reactions,” *Phys. Rev. A* **85**, 032707 (2012).
- [22] V. Giovannetti, S. Lloyd, and L. Maccone, “Advances in quantum metrology,” *Nat. Photon.* **5**, 222 (2011).
- [23] Y. S. Wang, C. Chen, and J. H. An, “Quantum metrology in local dissipative environments,” *New J. Phys.* **19**, 113019 (2017).
- [24] S. S. Szigeti, S. P. Nolan, J. D. Close, and S. A. Haine, “High-precision quantum-enhanced gravimetry with a Bose-Einstein condensate,” *Phys. Rev. Lett.* **125**, 100402 (2020).
- [25] C. Y. Luo, J. H. Huang, X. D. Zhang, and C. H. Lee, “Heisenberg-limited Sagnac interferometer with multiparticle states,” *Phys. Rev. A* **95**, 023608 (2017).
- [26] L. Pezzé and A. Smerzi, “Entanglement, nonlinear dynamics, and the Heisenberg limit,” *Phys. Rev. Lett.* **102**, 100401 (2009).
- [27] J. Joo, W. J. Munro, and T. P. Spiller, “Quantum metrology with entangled coherent states,” *Phys. Rev. Lett.* **107**, 083601 (2011).
- [28] W. T. He, H. Y. Guang, Z. Y. Li, R. Q. Deng, N. N. Zhang, J. X. Zhao, F. G. Deng, and Q. Ai, “Quantum metrology with one auxiliary particle in a correlated bath and its quantum simulation,” *Phys. Rev. A* **104**, 062429 (2021).
- [29] S. S. Zhou, M. Z. Zhang, J. Preskill, and L. Jiang, “Achieving the Heisenberg limit in quantum metrology using quantum error correction,” *Nat. Commun.* **9**, 78 (2018).
- [30] J. Ma, X. G. Wang, C. P. Sun, and F. Nori, “Quantum spin squeezing,” *Phys. Rep.* **509**, 89 (2011).
- [31] N. J. Engelsen, R. Krishnakumar, O. Hosten, and M. A. Kasevich, “Bell correlations in spin-squeezed states of 500 000 atoms,” *Phys. Rev. Lett.* **118**, 140401 (2017).
- [32] M. J. Holland and K. Burnett, “Interferometric detection of optical phase shifts at the Heisenberg limit,” *Phys. Rev. Lett.* **71**, 1355 (1993).
- [33] S. F. Huelga, C. Macchiavello, T. Pellizzari, and A. K. Ekert, “Improvement of frequency standards with quantum entanglement,” *Phys. Rev. Lett.* **79**, 3865 (1997).
- [34] A. W. Chin, S. F. Huelga, and M. B. Plenio, “Quantum metrology in non-Markovian environments,” *Phys. Rev. Lett.* **109**, 233601 (2012).
- [35] Y. Matsuzaki, S. C. Benjamin, and J. Fitzsimons, “Magnetic field sensing beyond the standard quantum limit under the effect of decoherence,” *Phys. Rev. A* **84**, 012103 (2011).
- [36] X. Y. Long, W. T. He, N. N. Zhang, K. Tang, Z. D. Lin, H. F. Liu, X. F. Nie, G. R. Feng, J. Li, T. Xin, Q. Ai, and D.-W. Lu, “Entanglement-enhanced quantum metrology in colored noise by quantum Zeno effect,” *Phys. Rev. Lett.* **129**, 070502 (2022).
- [37] S. Y. Bai and J. H. An, “Floquet engineering to overcome no-go theorem of noisy quantum metrology,” *Phys. Rev. Lett.* **131**, 050801 (2023).
- [38] A. Smirne, J. Kołodyński, S. F. Huelga, and R. Demkowicz-Dobrzański, “Ultimate precision limits for noisy frequency estimation,” *Phys. Rev. Lett.* **116**, 120801 (2016).
- [39] K. Macieszczak, “Zeno limit in frequency estimation with non-Markovian environments,” *Phys. Rev. A* **92**, 010102 (2015).
- [40] K. Yamamoto, S. Endo, H. Hakoshima, Y. Matsuzaki, and Y. Tokunaga, “Error-mitigated quantum metrology via virtual purification,” *Phys. Rev. Lett.* **129**, 250503 (2022).
- [41] W. Dür, M. Skotiniotis, F. Fröwis, and B. Kraus, “Improved quantum metrology using quantum error correction,” *Phys. Rev. Lett.* **112**, 080801 (2014).
- [42] I. Rojkov, D. Layden, P. Cappellaro, J. Home, and F. Reiter, “Bias in error-corrected quantum sensing,” *Phys. Rev. Lett.* **128**, 140503 (2022).
- [43] F. Reiter, A. S. Sørensen, P. Zoller, and C. A. Muschik, “Dissipative quantum error correction and application to quantum sensing with trapped ions,” *Nat. Commun.* **8**, 1822 (2017).
- [44] M. A. C. Rossi, F. Albarelli, D. Tamascelli, and M. G. Genoni, “Noisy quantum metrology enhanced by continuous nondemolition measurement,” *Phys. Rev. Lett.* **125**, 200505 (2020).
- [45] K. Bai, Z. Peng, H. G. Luo, and J. H. An, “Retrieving ideal precision in noisy quantum optical metrology,” *Phys. Rev. Lett.* **123**, 040402 (2019).
- [46] J. T. Shen and S. H. Fan, “Coherent single photon transport in a one-dimensional waveguide coupled with superconducting quantum bits,” *Phys. Rev. Lett.* **95**, 213001 (2005).



- [47] D. E. Chang, A. S. Sørensen, E. A. Demler, and M. D. Lukin, “A single-photon transistor using nanoscale surface plasmons,” *Nat. Phys.* **3**, 807 (2007).
- [48] L. Zhou, Z. R. Gong, Y. X. Liu, C. P. Sun, and F. Nori, “Controllable scattering of a single photon inside a one-dimensional resonator waveguide,” *Phys. Rev. Lett.* **101**, 100501 (2008).
- [49] L. Zhou, L. P. Yang, Y. Li, and C. P. Sun, “Quantum routing of single photons with a cyclic three-level system,” *Phys. Rev. Lett.* **111**, 103604 (2013).
- [50] L. Zhou, H. Dong, Y. X. Liu, C. P. Sun, and F. Nori, “Quantum supercavity with atomic mirrors,” *Phys. Rev. A* **78**, 063827 (2008).
- [51] Y.-X. Yao and Q. Ai, “Optical non-reciprocity in coupled resonators by detailed balance,” *Ann. Phys. (Berlin)* **535** (2023).
- [52] Z. H. Wang, L. Zhou, Y. Li, and C. P. Sun, “Controllable single-photon frequency converter via a one-dimensional waveguide,” *Phys. Rev. A* **89**, 053813 (2014).
- [53] K. Y. Bliokh, Y. P. Bliokh, V. Freilikher, S. Savel’ev, and F. Nori, “Colloquium: Unusual resonators: Plasmonics, metamaterials, and random media,” *Rev. Mod. Phys.* **80**, 1201 (2008).
- [54] H. P. Breuer and F. Petruccione, *The Theory of Open Quantum Systems* (Oxford University Press, USA, 2002).
- [55] P. Liu, P. Wang, W. Yang, G. R. Jin, and C. P. Sun, “Fisher information of a squeezed-state interferometer with a finite photon-number resolution,” *Phys. Rev. A* **95**, 023824 (2017).
- [56] Q. Ai and J. Q. Liao, “Quantum anti-Zeno effect in artificial quantum systems,” *Commun. Theor. Phys.* **54**, 985 (2010).